



# Dynamic Behavior of a Rotor-AMB System Due to Strong Base Motions

C. Jarroux<sup>1</sup>, J. Mahfoud<sup>1</sup>(✉), R. Dufour<sup>1</sup>, F. Legrand<sup>1</sup>, B. Defoy<sup>2</sup>,  
and T. Alban<sup>2</sup>

<sup>1</sup> Univ Lyon, INSA Lyon, CNRS UMR5259, LaMCoS, 69621 Lyon, France  
jarir.mahfoud@insa-lyon.fr

<sup>2</sup> GE Oil and Gas, 480 Avenue Gustave Eiffel, 71200 Le Creusot, France

**Abstract.** The paper investigates experimentally and numerically the nonlinear dynamics of a rotor supported by Active Magnetic Bearings (AMBs) and subjected to more or less severe motions from its support. In case of strong base excitations, the rotor can contact its touchdown bearings (TDBs) which are emergency bearings. The objective is to analyze the effect of the combination of mass unbalance forces, base motion excitations and contact nonlinearities on a rotor-AMB system response. The Finite Element method was used to model the on-board rotor. External force vectors and matrices with parametric coefficients related to the base motions appear in the equations of motion. The contact was modelled with a bilinear normal contact law and the tangential sliding friction effects are considered. Experiments were carried out on a lab-scale test rig that was mounted on a 6-axis shaker. At this stage, only harmonic base motions were considered. The numerical model was able to describe accurately the observed phenomena. AMBs were able to maintain the system under control, and the system remains stable even during the contact phase.

**Keywords:** Active Magnetic Bearings · Rotordynamics · Base motion  
Rotor-stator contact · Touchdown bearings

## 1 Introduction

Turbomachinery play a key role in the transformation, extraction or transport of the different types of available energies. Depending on the targeted applications, these machines may have to face more or less severe environmental conditions, such as turbomachinery used in nuclear plant when subjected to earthquake, as recently in Fukushima where the station was deeply damaged. The same behavior could be observed for Floating Production Storage and Offloading (FPSO) units used for the offshore production and storage of oil due to large waves or stormy events. Turbo-machines have to be able to withstand severe environmental conditions.

The base motion generates complex rotordynamics in particular in the case of deformable foundations or base rotations yielding parametric instabilities. At certain angular speed of the support, combined with the natural frequencies of the rotor, instability zones emerge and depend on the amplitude of the rotation angle [1–3]. When on-board rotors are supported by nonlinear bearings, complex dynamics are expected

[4, 5]. Depending on the amplitude of the applied sinusoidal base motion (translation or rotation), the rotor-bearing system exhibits periodic, quasi-periodic or even chaotic motions. Therefore, the dynamic behavior of on-board rotating machines should be carefully analyzed to improve the reliability and to maintain a maximal operability of the machines.

Active magnetic bearings (AMBs) are increasingly utilized in industrial applications for their many advantages such as frictionless support, no lubrication system, and a reduced footprint. They are inherently unstable, therefore a feedback control is needed and the PID is the most implemented controller in industrial applications [6]. Rotor-AMB systems are systematically equipped with touchdown bearings (TDBs) supporting the shaft when magnetic levitation is no more provided. In case of large displacements, contact between the rotor and the TDBs could occur leading to potential instabilities.

The use of magnetic forces can limit the effects of base motions. Several studies showed the effectiveness of AMBs to maintain the system stable [7–9]. However, in most cases, the amplitude of the rotor response due to the base motions was limited and interaction with TDBs was not generated. Few studies have considered this nonlinearity triggered by base motions while AMBs still operate. This could lead to dangerous rotordynamics such as backward whirl followed by dry whip instabilities [10].

This research project contributes to the improvement of knowledge concerning the dynamic behavior of turbomachinery supported by AMBs when subjected to external events. In particular, to investigate, numerically and experimentally, the dynamic behavior of a rotor-AMB system subjected to strong base motion leading the rotor to contact TDB while AMB still operate. The effects of flexible support was considered by other researchers [11], in this study the support is considered rigid.

First, the modelling approach is developed with the implementation of the rigid base motion inputs in the equations of motion. Then the experimental dispositive is described. The results obtained are shown and discussed at the end.

## 2 Numerical Model

The different models needed to perform transient simulations considering a rotor-AMB system subjected to external disturbances and potential TDB contacts are presented. The on-board rotor and the touchdown bearing models are described separately; the modelling approach is modular and each model can be either employed or not in the simulations.

### 2.1 On-Board Rotor

Usually, the rotor is composed of shaft, bearings, discs, and unbalance distribution, and here, the support is considered (Fig. 1). It is assumed that: the shaft is flexible and modelled by beam elements for lateral analysis; the discs are rigid and symmetric; the unbalance distribution is modelled by discrete masses and the support is rigid but mobile.

Lagrangian method is used. It consists in describing the motion of the rotor with respect to the rigid support R, as usually done in conventional rotordynamics studies [12], and the support motion with respect to the ground  $R_g$ , which is a Galilean frame. An intermediate frame is set-up to take into account the energy formulation of base motion inputs and to investigate the deflection of the rotor neutral line in the frame attached to the rigid support [13].

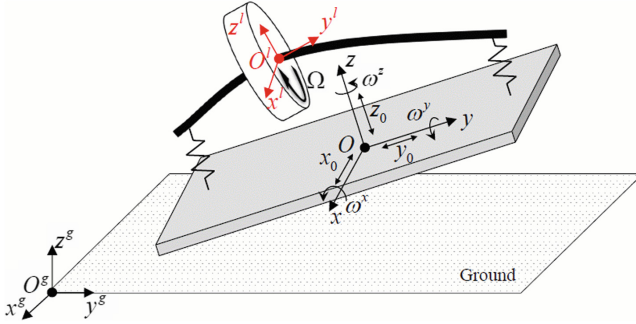


Fig. 1. On-board rotor frame

The Galilean frame  $R_g$  of center  $O_g$  is fixed and attached to the ground. The non-inertial frame  $R$  of center  $O$  is attached to the rigid base. And the local non-inertial frame  $R_1$  of center  $O_1$  is attached to the deflection line of the rotor. The frames of reference are first established and then vectors describing the different motions between each others are calculated. To derive the different energies of each components of the rotor, the instantaneous angular velocity vector and the position vector are needed. These vectors are expressed with respect to the Galilean frame  $R_g$  in the rigid support frame  $R$ . The energetic contribution and the virtual work of each components should be calculated: the flexible shaft contributes with the kinetic and strain energies; the discs with the kinetic energy; the discrete mass unbalances with the kinetic energy, and the bearing restoring forces with the virtual work.

The different contributions of the base are expressed in the frame associated with the rigid base in motion with respect to the Galilean frame. The base motions modify only the kinetic energies. Once the energies are set-up, they are derived by using the Lagrange's equations leading to the equations of motion as:

$$M\ddot{\delta} + \left(\Omega C^g + \omega^y C_{bm}^{\omega^y}\right)\dot{\delta} + \left(K^e + \dot{\omega}^y K_{bm}^{\omega^y} + \Omega \omega^y K_{bm}^{\Omega\omega^y} + \omega^{x2} K_{bm}^{\omega^{x2}} + \omega^{y2} K_{bm}^{\omega^{y2}} + \omega^{z2} K_{bm}^{\omega^{z2}} + \omega^x \omega^z K_{bm}^{\omega^x\omega^z}\right)\delta = F_{mu} + F_{bm} + F_g + F_{amb} + F_c \tag{1}$$

with  $M$ ,  $K^e$  and  $C^g$  are respectively the mass, the structural stiffness and the gyroscopic matrices.  $\Omega$  is the rotor rotational speed,  $\delta$ ,  $\dot{\delta}$ ,  $\ddot{\delta}$  are the rotor displacement, velocity and acceleration.  $F_{mu}$  is the mass unbalance force vector taking into account the normal centrifugal and tangential centripetal forces. The subscript  $bm$  stands for the base

motion effects. The external force vector  $F_{bm}$  contains all the contribution of the translations of the support combined with its rotations,  $F_g$  the effect of gravity,  $F_{amb}$  the forces delivered by the AMBs, which is the output of an augmented PID that takes into account the characteristics of the utilized AMBs. The model used is not developed in this paper.  $F_c$  represents the TDBs contact force vectors that will be developed in the next section.  $\omega^x; y; z$  is the rotational speed of the support along the direction x, y or z.  $C_{bm}^\omega$ ,  $K_{bm}^\omega$  are the additional (gyroscopic or stiffness) matrices due to the support rotations. Obviously, the support rotations introduce time-varying parametric excitations that could generate lateral instabilities.

## 2.2 TouchDown Bearing Model

TDBs have two main functions. The first one is to protect the AMBs from large unexpected transient loads that exceed the design capacity of AMBs. The second is to ensure a back-up support when AMBs are no longer available.

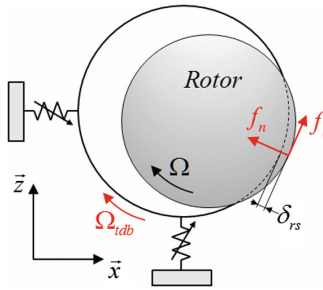


Fig. 2. TDB model

Usually, a ribbon damper is fitted between the outer race and the housing; it brings softness and damping when rotor-TDB interactions occur. TDBs generate contact forces in normal  $f_n$  and tangential  $f_t$  directions, as shown in Fig. 2. The normal component  $f_n$  is described by a contact law. Its mechanical expression is given by Eq. (2), where  $\delta_{rs}$  is the rotor-TDB relative clearance and  $\delta_{rd}$  is the ribbon crushing capacity.

$$f_n = \begin{cases} k_{brg}(\delta_{rs} - \delta_{rd}) + c_{brg}\dot{\delta} + k_{eq}\delta_{rd} & ; \delta_{rs} \geq \delta_{rd} \\ k_{eq}\delta_{rs} + c_{eq}\dot{\delta}_{rs} & ; \delta_{rd} > \delta_{rs} \geq 0 \\ 0 & ; \delta_{rs} > 0 \end{cases} \quad (2)$$

with  $k_{brg}$ ,  $c_{brg}$  the dynamic parameters of the ball bearing. When the rotor interacts with the TDB, it first contacts the coupled ball bearing ribbon damper system, considered in series mode. The related contact force is composed of the equivalent stiffness  $k_{eq}$  and damping  $c_{eq}$ . When the ribbon is fully crushed, meaning that  $\delta_{rs} \geq \delta_{rd}$  it only has a static contribution and the rotor faces the ball bearing stiffness. This model is characterized by softness and large damping when the ribbon is not crushed, then by a high stiffness and a low damping.

The tangential component  $f_t$  considers the sliding friction generated at the rotor-TDB interface due to different rotational speeds and considers the tangential damping provided by the ribbon damper counteracting the rotor whirl. The sliding friction is generated by using the regularized Stribeck model. The latter drives the TDB in rotation and  $\Omega_{tdb}$  represents its speed of rotation. An equivalent rotational inertia (balls and inner race) as well as a resistive torque are considered to compute this component.

The modelling approach that takes into account base motions, AMBs, mass unbalance, gyroscopic effects, gravity and contact with TDBs is schemed in Fig. 3.

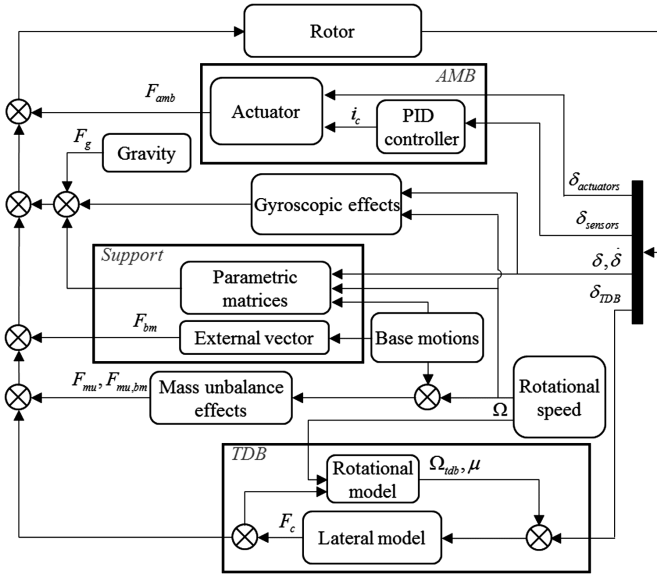


Fig. 3. Numerical model schema

The nonlinear contributions such as the additional forces due to the base motion (support block) or the efforts due to the contact of the rotor with the TDB (TDB block) are considered as restoring forces. It was the same concerning the forces delivered by the AMB (AMB block). The gravity as well as the gyroscopic effects were also considered in the second member of the equation of motion. This modelling approach is able to have a linear part concerning the rotor, consequently, the modal reduction can be applied easily [14].

The model developed enables system simulation in different configurations. For this work, only harmonic base motions were considered.

### 3 Experimental Model

The experiments were performed using an academic test rig, which is a commercial product manufactured by SKF® and was delivered with a dedicated PID controller. The test rig is equipped with two identical AMB called NDE (Non Drive End) and DE

(Drive End) bearings. Each bearing has a maximum static capability of 280 N with air gaps of 0.432 mm. The action lines are positioned in the configuration load between axes. They are powered in differential driving mode with a bias current of 1 A. Currents are provided in the range of 0–3A using PWM amplifiers. Two displacement sensors (variable reluctance probes) are integrated in the housing of each bearing and are non-colocalised with actuators.

The rotor is designed to obtain the dynamic behavior of high speed turbomachinery with a rigid shaft in the operating speed range and low gyroscopic effects. The rotor is made of standard steel, its mass is 6.5 kg and its length is 645 mm with a disc, 120 mm in diameter and 25 mm in thickness, placed at two-thirds of the bearing span from the DE side. The rotor is driven by a 500 W electric motor with a maximum speed of 12 600 rpm. The torque transmission is provided through a flexible coupling. The operating speed range is from 0 to 9 500 rpm (160 Hz), which includes the first two rigid modes. The rotational speed is measured by using a tachometer placed close to the motor. TDBs are cageless single row deep groove ball bearings with 0.1 mm clearance that was provided by the manufacturer.

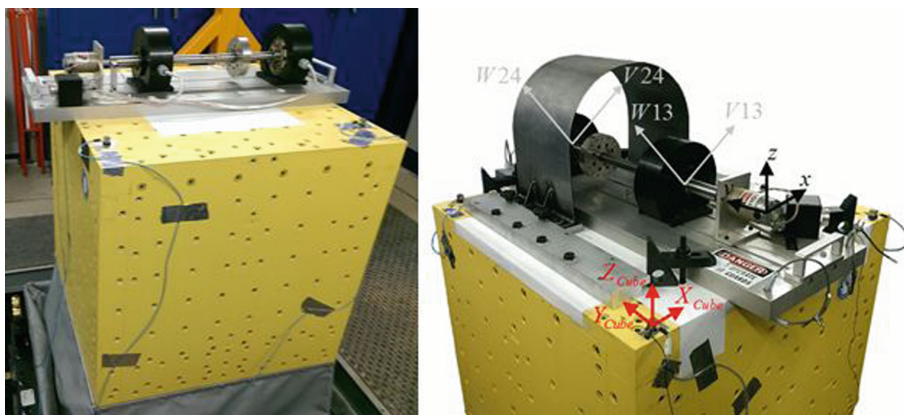


**Fig. 4.** Experimental test rig

To perform base motion tests, the academic test rig was mounted on a 6-axis hydraulic shaker as shown in Fig. 4 (the yellow cube). The shaker, provided by TEAM Corporation, is a fully integrated system. It has 6 real-time pilots able to apply various combinations of solicitations along and around the 3 axes (translations and rotations) to a maximum mass of 450 kg in a range [0–250] Hz. A maximum acceleration of 10 G,  $\pm 50$  mm in translation and  $\pm 4^\circ$  in rotation can be generated.

The data acquisition system of the shaker was used. Base accelerations were recorded in the three directions (Xcube, Ycube, Zcube) using four tri-axial accelerometers fixed on the shaker. The displacement and current sensors for each action line (V13, W13, V24, W24), and the rotational speed were also recorded. The sampling frequency was set to 24 756 Hz.

The tests were carried out in vertical translation, by using harmonic excitations. For all the configurations tested, the same level of mass unbalance was applied; 32 g.mm at 0 degree that corresponds to four times the recommended unbalance by the API standards. The support motion was a 20 Hz sine translation ranging from 0.1 to 1.1 G. The chosen frequency and amplitude represent the best frequency range to exhibit TDB contact phenomena. The rotor rotational speed was set to 6 000 rpm. To smoothly trigger the rotor-TDB contact, the acceleration level targeted by the shaker is set-up progressively enabling reduced overshoot. This phase of operation lasted almost 30 s. Once reached, the shaker motion was maintained for approximately 40 s to catch potential onset of nonlinear dynamic regimes. The excitation signals were not purely sinusoidal, the contribution of the shaker operating frequencies were present. During the different test configurations, AMBs were kept operational. The shaker stop was also recorded to check and analyze the capacity of the controller and the AMBs to center and to control the rotor after severe contact situations.

## 4 Results

Measured and predicted rotor vertical displacements were compared. The accelerations recorded on the shaker were implemented in the numerical model.

First, the results obtained are analyzed for the whole test duration then, a zoom on ten periods using orbit plots provides better insights into the involved phenomena. Figure 5 shows the predicted and measured rotor displacements in vertical direction for a rotating speed of 6 000 rpm and subjected to a progressively increased acceleration of the shaker up to 1.1 G. The dotted lines represent the TDBs at both DE and NDE.

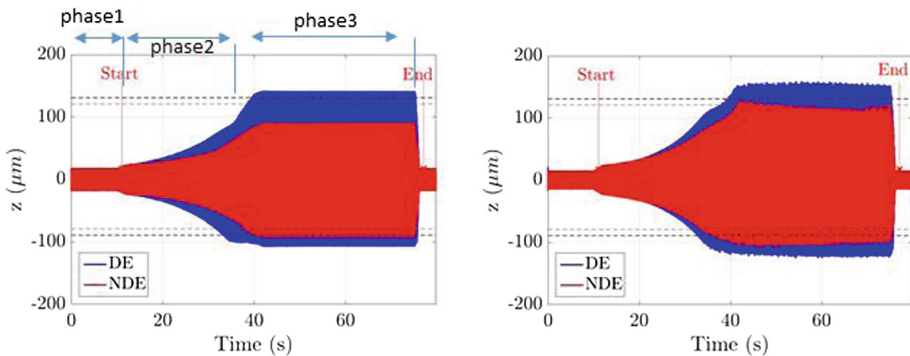


**Fig. 5.** Predicted (a) and measured (b) vertical displacements, 6 000 rpm, 0–1.1 G, 20 Hz

The base motion starts close to 10 s and contact occurred close to 35 s. The measured vertical responses seem to be described qualitatively well by the numerical model. The controller manages the unbalance forces combined with base motions and TDB contacts. Once the shaker stops, the rotor quickly recovers its centered position in both predictions and measures.

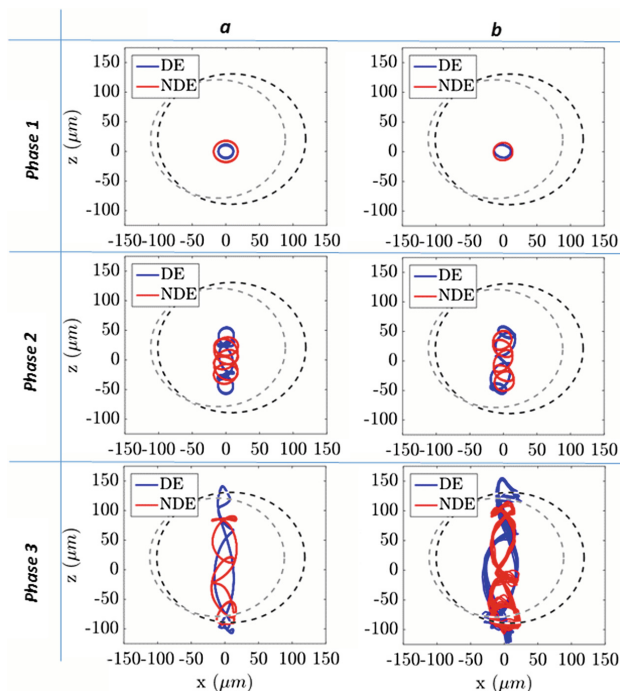


**Fig. 6.** Predicted (a) and measured (b) orbits, 6 000 rpm, 0–1.1 G, 20 Hz

As the acceleration level was set-up progressively, orbit plots permit analyzing the combined effects of mass unbalance and base motion loads for cases without or with TDB interactions. In Fig. 6, the orbits during the different phases were analyzed. For each phase, the last ten periods according to the base motion frequency were presented. At phase 1 (recorded results at 5 s), the shaker was shut down and only the mass unbalance forces were present. The orbits obtained were relatively circular (symmetric system), and the amplitude is largely smaller than the TDB clearance. Then during phase 2, the excitation level was increased progressively from 0 to 1.1 G (recorded results at 28.6 s, when the acceleration level equals 0.3 G). It could be noticed that the model describes closely the phenomena observed. Here, no contact between the rotor and the TDBs, and typical combinations of vertical base motion, unbalance forces were exhibited. Orbits were periodic due to integer ratio between the rotor speed and the excitation frequency. During phase 3, the highest level was maintained (recorded results at 60.7 s and 1.1 G acceleration level). The predicted and measured orbits were close. Rotor-TDBs interactions were generated and the periodicity of orbits was conserved with respect to the non-contacting case. Orbit shapes were flattened and the rotor had mainly forward whirl, indicating weak sliding friction effects. This could be due to the fact that the TDBs were driven in rotation and therefore, the sliding friction coefficient was small at the rotor-TDB interface.

Finally, the AMBs remained stable in both numerical and experimental analysis. The model is able to correctly describe the combination of base motion, mass unbalance, AMBs and TDBs contacts generating complex dynamics.



Measured orbits are slightly tilted and this may be related to small discrepancies in the proximity sensor sensitivity. The global measured energetic level of vibrations is higher than the predicted one since the acceleration signals were filtered before being implemented in the model. Moreover, the vibrations coming from the foundation were not considered in the numerical model since the support is assumed infinitely rigid. However, the model describes closely the main observed phenomena.

## 5 Conclusions

The aim was to investigate experimentally and numerically the nonlinear dynamics of a rotor supported by Active Magnetic Bearings and subjected to severe motions from its support. The test configurations were chosen to be representative of real turbomachines operating conditions. The PID controller was tuned for conventional operating conditions, and no specific work on the control loop was done. The aim was to check if the control could be able to withstand the nonlinearities due to the contact.

The model was able to reproduce the overall dynamics and the main observed phenomena considering an academic on-board rotor-AMB system.

Even if the PID controller was tuned without considering this particular excitation, the controller remains globally stable in both numerical and experimental tests. No dry whip instabilities were noticed in both experimental and numerical investigations. Orbit shapes were flattened and the rotor has mainly forward whirl, indicating weak sliding friction effects. The behavior observed may indicate that the TDBs were driven in rotation reaching the rotor rotational speed during harmonic tests; therefore, tangential friction effects were limited.

Even if the model of the AMB and the controller were not presented, we observed that the restoring magnetic forces generated by actuators remained in an acceptable linear range. Neither AMB nonlinearities nor amplifier saturation were exhibited in both predictions and measures. The dynamic capacity of the AMBs are oversized considering the test rig. We are now investigating the same behavior by using adapted dynamic capacity.

This numerical validation provides confidence considering the prediction of the dynamic behavior of on-board industrial turbomachinery.

**Acknowledgements.** This work was supported by the French National Agency of Research and Technology (ANRT) [CIFRE grant number: 2013/1376] and by French National Research Agency (ANR) Equipex PHARE 10-EQPX-0043.

## References

1. Driot, N., Lamarque, C.H., Berlioz, A.: Theoretical and experimental analysis of a base-excited rotor. *J. Comput. Nonlinear Dyn.* **1**, 257–263 (2006)
2. Duchemin, M., Berlioz, A., Ferraris, G.: Dynamic behavior and stability of a rotor under base excitation. *J. Vib. Acoust.* **128**, 576–585 (2006)

3. Han, Q., Chu, F.: Parametric instability of flexible rotor-bearing system under time-periodic base angular motions. *Appl. Math. Model.* **39**, 4511–4522 (2015)
4. Dakel, M., Baguet, S., Dufour, R.: Nonlinear dynamics of a support-excited flexible rotor with hydrodynamic journal bearings. *J. Sound Vibr.* **333**(10), 2774–2799 (2014)
5. El-Saeidy, F.M.A., Sticher, F.: Dynamics of a rigid rotor linear/nonlinear bearings system subject to rotating unbalance and base excitations. *J. Vibr. Control* **16**, 403–438 (2010)
6. Schweitzer, G., Maslen, E.H.: *Magnetic Bearings, Theory, Design, and Application to Rotating Machinery*. Springer, Heidelberg (2009)
7. Das, A.S., Dutt, J.K., Ray, K.: Active vibration control of unbalanced flexible rotor-shaft systems parametrically excited due to base motion. *Appl. Math. Model.* **34**(9), 2353–2369 (2010)
8. Cole, M.O.T., Keogh, P.S., Burrows, C.R.: Vibration control of a flexible rotor/magnetic bearing system subject to direct forcing and base motion disturbances. *Proc. Inst. Mech. Eng. Part C: J. Mech. Eng. Sci.* **212**(7), 535–546 (1998)
9. Hawkins, L.A., Murphy, B., Zierer, J., Hayes, R.: Shock and vibration testing of an AMB supported energy storage flywheel. *JSME Int. J. Ser. C Mech. Syst. Mach. Elements Manuf.* **46**(2), 429–435 (2003)
10. Bartha, A.R.: Dry friction backward whirl of rotors. Ph.d. dissertation, ETH, Zurich (2000)
11. Cavalca, K.L., Cavalcante, P.F., Okabe, E.P.: An investigation on the influence of the supporting structure on the dynamics of the rotor system. *Mech. Syst. Sig. Process.* **19**(1), 157–174 (2005)
12. Lalanne, M., Ferraris, G.: *Rotordynamics Prediction in Engineering*. Wiley, Hoboken (1998)
13. Jarroux, C.: Nonlinear transient dynamics of on-board rotors supported by active magnetic bearings. Ph.D. dissertation, INSA Lyon, Lyon (2017)
14. Defoy, B., Alban, T., Mahfoud, J.: Assessment of the effectiveness of a polar fuzzy approach for the control of centrifugal compressors. *ASME J. Dyn. Syst. Measur. Control* **136**, 041004-1–041004-8 (2014)